

# Fault-tolerant quantum repeater with atomic ensembles and linear optics

Zeng-Bing Chen,<sup>1,2,\*</sup> Bo Zhao,<sup>1,2</sup> Jörg Schmiedmayer,<sup>2</sup> and Jian-Wei Pan<sup>1,2,†</sup>

<sup>1</sup>*Hefei National Laboratory for Physical Sciences at Microscale and Department of Modern Physics, University of Science and Technology of China, Hefei, Anhui 230026, China*

<sup>2</sup>*Physikalisches Institut, Universität Heidelberg, Philosophenweg 12, D-69120 Heidelberg, Germany*

Recent years have witnessed remarkable experimental progresses on photon manipulation<sup>1,2,3</sup> for quantum communication (QC). However, current probabilistic entangled photon sources and the difficulty of storing photons limit these experiments to moderate distances (about 10-100 km for quantum cryptography<sup>4</sup>) and a few photonic qubits. For long-distance ( $\sim 10^3$ - $10^4$  km) QC, one must realize quantum network with many communication nodes via the quantum repeater (QR) protocol<sup>5</sup>. The existing implementations<sup>6,7,8</sup> of QR seem to be not enough. Here we propose an efficient, fault-tolerant long-distance QC architecture with linear-optical robust entangler and atomic-ensemble-based quantum memory<sup>9,10</sup> for photonic polarization qubits; the architecture is based on two-photon interference, which is about  $10^8$  times more stable than single-photon interference (as used in refs. 6,7) for atomic-ensemble-based single photons. Incorporating several significant recent advances on atomic-ensemble-based techniques<sup>9-18</sup> and linear-optical entanglement purification<sup>3</sup>, our scheme faithfully implements QR and thus enables a realistic avenue for relevant experiments with many photons.

QC ultimately aims at absolutely secure transfer of classical messages by means of quantum cryptography<sup>4</sup> or faithful teleportation of unknown quantum states<sup>19</sup>. Photons are ideal quantum information carriers for QC. Unfortunately, photon losses and the decrease in the quality of entanglement (decoherence) scale exponentially with the length of the communication channel. The QR protocol<sup>5</sup> combining entanglement swapping<sup>2,20</sup> and purification<sup>3,21</sup> enables to establish high-quality long-distance entanglement in the communication time increasing only polynomially with transmission distance. Quantum memory is crucial for ensuring polynomial scaling in the communication efficiency as all entanglement purification protocols must be probabilistic.

Duan *et al.* (DLCZ)<sup>6</sup> proposed an original implementation of QR by using atomic ensembles (AEs) as local memory qubits. This elegant scheme was believed to have built-in entanglement purification. Unfortunately, the single-photon interference at photodetectors, used in the DLCZ protocol (see also ref. 7) for entanglement creation and connection, has to be stabilized at a length scale well below the wavelength of single photons. For instance, to maintain path length phase stabilities at the level of  $\lambda/10$  ( $\lambda$ : wavelength; typically  $\lambda \sim 1 \mu\text{m}$  for single photons generated from AEs<sup>16</sup>) requires the fine control of timing jitter at a sub-femtosecond level, which is almost an experimentally forbidden technique as compared with the lowest reported jitter even for kilometer-scale distances<sup>22</sup>. This phase-stability problem could be overcome by interfering two photons, e.g., for ion-cavity system<sup>23</sup>. However, this improved robust entanglement creation is unscalable to many communication nodes. In other attractive protocols<sup>7,8</sup> it remains to be seen if local collective operations can be done with high precision which is required for implementing QR. Up to date, only linear optics provides the experimentally demonstrated precision<sup>3</sup> required by the QR protocol.

In recent years, several exciting ideas of using AEs in quantum information processing were proposed, such as quantum memory<sup>9,10</sup> and nearly ideal photon counting<sup>24,25</sup>. In the efforts of realizing the AE-based QR protocol<sup>6</sup>, significant experimental advances<sup>11,12,13,14,15,16,17,18</sup> have been achieved recently. Based on these theoretical and experimental breakthroughs, here we present a robust and faithful implementation of QR for efficient long-distance QC with linear optics manipulating flying photonic qubits and AEs as localized memory qubits; the time overhead scales polynomially with the communication length.

A crucial component of our architecture is quantum memory for photonic polarization qubits (see Fig. 1 and Methods section). Importantly, our quantum memory works even when the two probability amplitudes in the stored state  $\alpha|R\rangle + \beta|L\rangle$  are not c-numbers but quantum states of other photonic qubits. As a result, two memories as in Fig. 1 can be deterministically entangled in their ‘polarizations’  $|r\rangle$  and  $|l\rangle$  by storing two polarization-entangled photons, e.g.,  $\frac{1}{\sqrt{2}}(|r\rangle|r\rangle + |l\rangle|l\rangle) \leftrightarrow \frac{1}{\sqrt{2}}(|R\rangle|R\rangle + |L\rangle|L\rangle)$ . The latter are entangled by a deterministic polarization-entangler using four single photons, linear optics and an event-ready detection (see Supplementary Information). With an overall success probability of  $p_1 = \frac{1}{8}$  for perfect photon counting, such an ‘event-ready’ entangler can deterministically generate two maximally polarization-entangled qubits.

However, in the above entanglement creation mechanism, if the two memories are remotely located, the photon loss experienced in the transmission of the entangled photon pairs is significant, rendering the entanglement creation for two remote memories non-deterministic. To overcome this problem (see Fig. 2a), one can first create deterministically each pair of maximally entangled memories at two adjacent communication nodes (nodes  $i$  and  $i+1$ ) as the photon

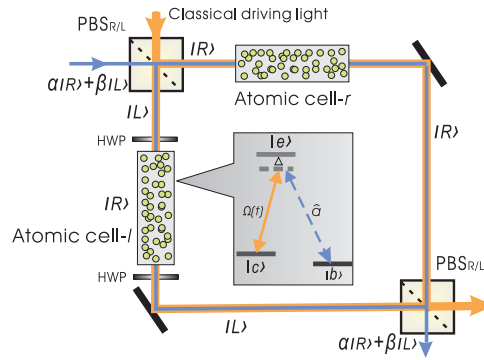


FIG. 1: **Quantum memory for photonic polarization qubits.** Two identical ensembles are identically driven by a classical field, which is equally right- and left-circularly polarized. Classical and quantized light fields are feed into the first  $\text{PBS}_{R/L}$  ('rotated' PBS which reflects left-circular photons and transmits right-circular photons) and will leave at two different outputs of the second  $\text{PBS}_{R/L}$ . Two half-wave plates (HWP) functioning as  $|R\rangle \leftrightarrow |L\rangle$  are placed along the  $|L\rangle$ -output of the first  $\text{PBS}_{R/L}$ . As the atomic cell- $r$  (cell- $l$ ) works as quantum memory for single photons with right-circular (left-circular) polarization via the adiabatic transfer method, the whole setup is then quantum memory of any single-photon polarization states. The inset shows the relevant level structure of the atoms, with the ground state  $|b\rangle$ , the metastable state  $|c\rangle$  for storage, and the excited state  $|e\rangle$ . The  $|c\rangle$ - $|e\rangle$  transition is coherently driven by the classical field of Rabi frequency  $\Omega(t)$ , and the  $|b\rangle$ - $|e\rangle$  transition is coupled to a quantized light field  $\hat{a}$  with a coupling constant  $g$ . The two detunings for the two transitions are both equal to  $\Delta$  (the two-photon resonance).

losses can be safely neglected at each node. Then the two photons stored in the two up memories are simultaneously retrieved and subject to a Bell-state measurement (BSM) at the middle point (entanglement swapping). Conditioned on the result of this BSM, the remaining two memories, located at nodes  $i$  and  $i + 1$ , are maximally entangled in a deterministic way (i.e., event-ready). With linear-optical BSM, the time needed for this to occur is  $T_{ent} = \frac{T_0 + 2T_{cc}}{p_e}$ . Here  $p_e = \frac{1}{2}e^{-L_0/L_{att}}$  is the success probability of the BSM by taking into account the channel attenuation;  $T_{cc} = \frac{L_0}{c}$  is the classical-communication time between nodes  $i$  and  $i + 1$  and  $T_0$  the entanglement preparation time at a single node.

To implement the QR protocol<sup>5</sup>, one divides the whole communication channel into many segments, each of which has a length  $L_0$  comparable to the channel attenuation length  $L_{att}$ . Entanglement across all segments is first generated in parallel using the above entanglement creation protocol. The communication length of the original segments can be extended by entanglement connection shown in Fig. 2b.

With imperfect entanglement and erroneous local operations, entanglement connection, together with decoherence, will reduce the fidelity of entanglement<sup>5</sup>. Then at certain stage of entanglement connection, the less entangled states have to be purified via the entanglement purification protocol<sup>3,21</sup> to enable further entanglement connection. Figure 2c shows how to achieve linear-optical entanglement purification between any specified two nodes, e.g., node- $i$  and node- $j$ , across which one has two less entangled pairs of quantum memories.

By combining quantum memory for photonic polarization qubits, linear-optical entanglement connection and purification, our scheme provides a faithful physical implementation of the QR protocol<sup>5</sup>. An alternative entanglement creation mechanism without the deterministic feature is also proposed for the same purpose by directly extending the DLCZ scheme (Zhao, B. *et al.*, unpublished). Below we further demonstrate that the efficiency of our scheme scales polynomially with the communication distance  $\ell$ .

To this end, we estimate the time for realizing the 'nested entanglement purification'<sup>5</sup>. Suppose  $\mathcal{N} \equiv \ell/L_0 = k^z$  and  $k = 2^l$  ( $z, l$ : integer) entangled pairs of fidelity  $F_e$  are created in parallel between A and  $C_1, C_1$  and  $C_2, \dots, C_{\mathcal{N}-1}$  and B by entanglement swapping within time  $T_{ent}$ . We first connect the entangled pairs at all nodes except  $C_k, C_{2k}, \dots, C_{\mathcal{N}-k}$  by BSM at local nodes, resulting in  $\mathcal{N}/k$  pairs of length  $k$  (which corresponds to communication distance  $kL_0$ ) and fidelity  $F_k$  between A and  $C_k, C_k$  and  $C_{2k}, \dots, C_{\mathcal{N}-k}$  and B. The integer  $k$  is chosen such that  $F_k > F_{\min} > \frac{1}{2}$  to enable further purification. In parallel fashion we construct  $2^K$  copies to purify these new pairs. After purification, we obtain one pair of fidelity  $\geq F_e$  on each of these new segments. We iterate the procedure until the  $z$ -th level. The total time  $T_{tot}$  needed to implement the nested purification can be calculated after a lengthy algebra (see Supplementary Information). If  $T_{op}$  (the local operation time) and  $T_0$  are not too large, the main contribution to  $T_{tot}$  is dominated

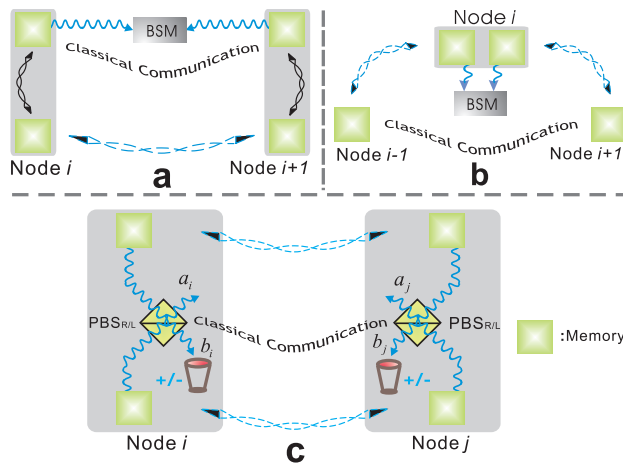


FIG. 2: **Setups for entanglement creation, connection and purification.** **a**, At two adjacent communication nodes, nodes  $i$  and  $i + 1$ , two pairs of memory qubits are first entangled by storing the event-ready entanglement of two photons. Then the two photons stored in the up memory qubits at the two nodes are simultaneously retrieved and subject to a BSM at the middle point. This entanglement swapping process will deterministically entangle the two down memory qubits which are spatially separated to a distance  $L_0$ . The resulting entanglement is robust in the sense that it does not depend on the phases that single photons would acquire as they propagate along a long distance<sup>23</sup>. **b**, Two well entangled pairs of memory qubits, one across nodes  $i - 1$  and  $i$  and another across nodes  $i$  and  $i + 1$ , are prepared in parallel. The BSM on the two photons released simultaneously from the two memories at node  $i$  results in, with a probability of  $\frac{1}{2}$ , well entangled quantum memories across nodes  $i - 1$  and  $i + 1$  in a definite Bell state. The entanglement is thus connected up to the communication distance  $2L_0$ . **c**, Entanglement purification between any specified two nodes (node- $i$  and node- $j$ ) across which two pairs of memory qubits are less entangled. After the simultaneous retrieval of the four single photons stored in the four memory qubits, the two photons at each node are incident simultaneously on the PBS at that node. Then one uses the linear-optics entanglement purification protocol (as realized recently<sup>3</sup>). After a successful purification photons in modes  $a_i$  and  $a_j$  are more entangled and then stored in corresponding memories for future operations.

by the classical communication and approximated by

$$T_{tot} \sim 2T_{cc} p_e^{-1} p_{\text{BSM}}^{-z\ell} \prod_{m=1}^z \prod_{i=1}^K p_{mi}^{-1} \quad (1)$$

Here  $p_{\text{BSM}} = \frac{1}{2}$  is the success probability of BSM at local nodes;  $p_{mi}$  ( $1/4 < p_{mi} < 1/2$ ) is the success probability of the  $i$ th purification for the  $m$ th nesting level and depends on the fidelity of states before the  $i$ th purification. Finally, we can get between A and B an entangled pair with fidelity  $\geq F_e$ . The total number of consumed entangled pairs is  $R = 2\mathcal{N}^{\log_k 2^K + 1} = 2(\ell/L_0)^{\log_k 2^K + 1}$ . It is easy to see that both the resources and total time for establishing the high-fidelity entangled pair between A and B grow polynomially with the distance  $\ell$ .

All the entanglement creation, connection and purification in our scheme rely on two-photon interference. The AE-based single photon generation<sup>15,16</sup> makes use of the electromagnetic-induced transparency<sup>16</sup> which is characterized by narrow spectral transparency window. Single photons generated this way have a large coherence time at about 100 ns (or coherence length of about 30 m). As a result, nearly perfect temporal and spatial overlapping to ensure good long-distance two-photon interference can easily be achieved at this length scale. In the DLCZ scheme relying on single-photon interference, phase stabilities should be maintained on the order of sub-wavelength ( $\sim 100$  nm) of single photons. In this sense, our scheme is thus about  $10^8$  times more robust in maintaining long-distance phase stabilization than the DLCZ scheme and will significantly facilitate the experimental implementation of the AE-based quantum network.

The QR protocol can tolerate faulty local operations in the few-percent region<sup>5</sup>, which in our scheme can easily be outperformed by current linear-optical elements<sup>3</sup> manipulating single photons of long coherence length. The utility of two-photon interference and active entanglement purification by linear optics thus enable fully robust and fault-tolerant long-distance QC. With distant well entangled quantum memories, long-distance entanglement-based communications can simply be implemented as the stored photonic polarization qubits can be retrieved on demand and then subject to further operations, e.g., arbitrary single-qubit operations and BSM, which can all be done with simple linear optical elements.

Now let us consider several practical factors for realizing our proposal. Recent years have witnessed significant experimental and theoretical progresses on the techniques relevant to our scheme. Controllable generation, storage and retrieval of single photons with tunable frequency, timing and bandwidth have been demonstrated<sup>15,16,17,18</sup> based on the DLCZ protocol. In refs. 17,18 a deterministic single-photon source was demonstrated using measurement-based feedback protocol. Note that our entanglement creation efficiency shows a novel memory-enhanced feature by using AE-based, heralded single photons (see Supplementary Information).

A long storage time is crucial for implementing our QR protocol. Storage time of up to 30  $\mu\text{s}$  was reported recently in ref. 17. An optical dipole trap may have the potential to extend the storage time to 1 second<sup>26</sup>. According to a recent proposal<sup>27</sup>, quantum memory with nuclear atomic spins might have very long storage time of about hours.

One of the major factors affecting the efficiency of our scheme is single-photon detection. Fortunately, based on the same AE-based quantum memory technique, high-efficiency ( $> 99\%$ ) photon counting<sup>24,25</sup> is feasible by using quantum state transfer and state-selective fluorescence detection with nearly unit efficiency. Using AE-based photon counting, we can estimate  $T_{tot}$  and resources to create an entangled pair across the distance 1280 km using the simplest nesting procedures with  $l = K = 1$ ,  $k = 2^1$ ,  $\mathcal{N} = 2^7$  and  $L_0 = 10$  km (i.e.,  $T_{cc} = 33 \mu\text{s}$ ). The local operations and initial preparation are considered to be performed in  $T_{op} = T_0 = 10 \mu\text{s}$  and the photon loss rate is about 0.1 dB/km. The entanglement swapping and connection are always performed with the working state  $F \left| \phi_{R/L}^+ \right\rangle \left\langle \phi_{R/L}^+ \right| + (1-F) \left| \psi_{R/L}^+ \right\rangle \left\langle \psi_{R/L}^+ \right|$ , where  $\left| \phi_{R/L}^+ \right\rangle = \frac{1}{\sqrt{2}}(|R\rangle |R\rangle + |L\rangle |L\rangle)$  and  $\left| \psi_{R/L}^+ \right\rangle = \frac{1}{\sqrt{2}}(|R\rangle |L\rangle + |L\rangle |R\rangle)$ . We assume the initial fidelity  $F = 0.88$  of the adjacent entangled memories in Fig. 2a, as can be estimated by connecting two adjacent memories from two pairs of photon-memory entanglement of fidelity 0.94 after 5 km free-space transmission<sup>28</sup> of both photons (see Fig. 2a). Our numerical calculation gives the total time  $T_{tot}$  of about 10 s, the total resources of about  $3 \times 10^4$  and a final entangled pair with fidelity  $\sim 0.98$ . Such a high fidelity stems from the fact that the purification scheme in our proposal is efficient<sup>3</sup>. We also note that the time overhead can be significantly reduced by optimization.

Besides decoherence, another source of errors is photon losses. Decoherence and photon losses in transmission can be overcome in our scheme, as shown above. However, photon losses could also be caused, e.g., by nonideal photon detections and inefficiency of retrieving photons from quantum memory. Remarkably, further analysis shows that our scheme is still polynomially efficient for such photon losses and thus completely photon-loss tolerant (see Supplementary Information). Yet, the AE-based photon counting and well-behaved quantum memory, still under intensive development, are two key techniques which will greatly help the realistic long-distance QC.

Our fault-tolerant QR protocol exploits the advantages of both linear optics manipulating photons with very high accuracy and AEs as quantum memory. At the interface of AEs and photons, we can integrate within our proposal the existing linear-optical quantum protocols and AE-based schemes on photon storage and high-efficiency photon counting into a single unit. This would allow us to realize all ingredients required for long-distance QC. As we will report elsewhere, the robust entanglement creation mechanism can be used to entangle a complex multi-party quantum network for efficient one-way quantum computing with cluster states<sup>29</sup>. Such an AE-based quantum network provides an exciting perspective for manipulating a large number of photons for applications ranging from multiparty quantum information protocols to fundamental quantum experiments. While our scheme is specified to AEs, the general mechanism can also be applied to other light-matter (e.g., trapped atoms/ions or solid-state devices) interfaces.

## Methods

### Quantum memory for photonic polarization qubits

The AE-based quantum memory<sup>9,10</sup> consists of a coherently driven AE ( $N \gg 1$  atoms) of large optical thickness with the level structure shown in the inset of Fig. 1. The whole system may have particular zero-energy eigenstates, the so-called ‘dark states’ which represent elementary excitations of bosonic quasiparticles, i.e., the dark-state polaritons. The single-polariton state is  $|D, 1\rangle \equiv \frac{\Omega(t)}{\sqrt{\Omega^2(t)+g^2N}} |1\rangle |\mathbf{b}\rangle - \frac{g\sqrt{N}}{\sqrt{\Omega^2(t)+g^2N}} |0\rangle |c^1\rangle$ . Here  $|0\rangle$  ( $|1\rangle$ ) is the vacuum (single-photon) state of the quantized field,  $|\mathbf{b}\rangle = \bigotimes_i^N |b\rangle_i$ ,  $|c^1\rangle \equiv \frac{1}{\sqrt{N}} \sum_i^N |c\rangle_{ii}$  ( $|b\rangle |\mathbf{b}\rangle$ ) is the collective single-excitation atomic state. Quantum memory works by adiabatically changing  $\Omega(t)$  such that one can coherently map  $|D, 1\rangle$  onto either purely atom-like state  $|0\rangle |c^1\rangle$  where the single photon is stored, or purely photon-like state  $|1\rangle |\mathbf{b}\rangle$ , which corresponds to the release of the single photon in  $|1\rangle$ . In principle, quantum memory based on this adiabatic transfer method is reversible, preserves pulse shape of the stored single photons (as shown in ref. 10 by going beyond the simple single-mode case) and may have efficiency very close to unity. The original quantum memory was proposed for storing a coherent superposition of photon-number states; two AEs can be entangled by storage of two entangled light fields<sup>9</sup>.

However, here we need quantum memory for photonic polarization qubits, which is more robust as compared with other implementations of photonic qubits. Figure 1 shows quantum memory for storing any single-photon polarization states. For definiteness, let us suppose that the atomic cell- $r$  (cell- $l$ ) in Fig. 1 can achieve quantum memory for single-photon state  $|R\rangle \equiv |1_R, 0_L\rangle = |1_R\rangle \otimes |0_L\rangle$  with right-circular polarization ( $|L\rangle \equiv |0_R, 1_L\rangle = |0_R\rangle \otimes |1_L\rangle$ ) with left-circular

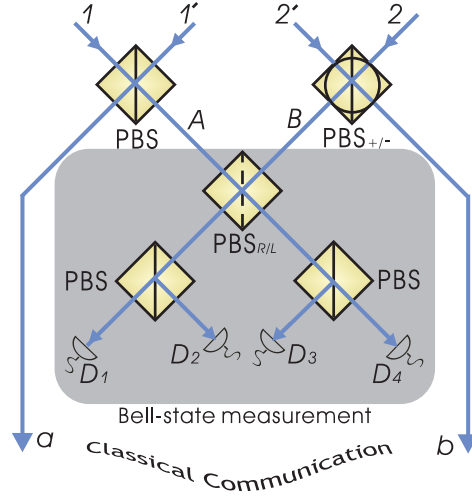


FIG. 3: **Deterministic single-photon polarization entangler.** PBS (PBS<sub>+/-</sub>; PBS<sub>R/L</sub>) reflects photons with vertical-polarization  $|V\rangle$  ( $|-\rangle$ -polarization;  $|L\rangle$ -polarization) and transmits photons with horizontal-polarization  $|H\rangle$  ( $|+\rangle$ -polarization;  $|R\rangle$ -polarization). Here  $|\pm\rangle = \frac{1}{\sqrt{2}}(|H\rangle \pm |V\rangle)$  and  $|R/L\rangle = \frac{1}{\sqrt{2}}(|H\rangle \pm i|V\rangle)$ . The four single photons are prepared on demand in an initial state  $|-\rangle_1 |V\rangle_2 |+\rangle_{1'} |H\rangle_{2'}$ . After passing through the first PBS and PBS<sub>+/-</sub>, one selects, with the probability of 1/4, the ‘four-mode’ case where there is one and only one photon in each of the four output modes ( $a, b; A, B$ ). Then the Bell-state measurement (BSM) on photons  $A$  and  $B$  will collapse photons  $a$  and  $b$  into a definite Bell state conditioned on the result of the BSM. In our case, a coincidence count between single-photon detectors  $D_1$  and  $D_4$  ( $D_1$  and  $D_3$ ) or between  $D_2$  and  $D_3$  ( $D_2$  and  $D_4$ ) leaving photons along paths  $a$  and  $b$  deterministically entangled in  $|\phi_{ab}^-\rangle_{R/L}$  ( $|\phi_{ab}^+\rangle_{R/L}$ ), with the Bell states  $|\phi_{ab}^\pm\rangle_{R/L} = \frac{1}{\sqrt{2}}(|R\rangle|R\rangle \pm |L\rangle|L\rangle)$ .

polarization) via the adiabatic transfer method described above, namely,

$$|D_{r/l}, R/L\rangle \rightarrow \begin{cases} |R/L\rangle |\mathbf{b}_{r/l}\rangle, & \text{for } \Omega(t) \gg g\sqrt{N} \\ |0_{R/L}\rangle |c_{r/l}^1\rangle, & \text{for } \Omega(t) \ll g\sqrt{N} \end{cases} \quad (2)$$

by adiabatically changing  $\Omega(t)$ . Here  $|D_r, R\rangle$  ( $|D_l, L\rangle$ ) is the single-polariton state of the cell- $r$  (cell- $l$ ), and  $|c_r^1\rangle \equiv |r\rangle$  ( $|c_l^1\rangle \equiv |l\rangle$ ) the single-excitation atomic state of cell- $r$  (cell- $l$ ).

The above quantum state transfer is a linear reversible process. Then the proposed setup in Fig. 1 works as a quantum memory of any single-photon polarization state described by the density operator  $\rho_p = \sum_{i,j=R,L} p_{ij} |i\rangle \langle j|$  (pure or mixed), namely,  $\rho_p \otimes |\mathbf{b}_r\rangle \langle \mathbf{b}_r| \otimes |\mathbf{b}_l\rangle \langle \mathbf{b}_l| \leftrightarrow |0_R\rangle \langle 0_R| \otimes |0_L\rangle \langle 0_L| \otimes \sum_{\alpha,\beta=r,l} p_{\alpha\beta} |\alpha\rangle \langle \beta|$ . Here  $|c_r^1\rangle |\mathbf{b}_l\rangle \equiv |r\rangle$  and  $|\mathbf{b}_r\rangle |c_l^1\rangle \equiv |l\rangle$ . Two AEs being a quantum memory for polarization qubits at each node are thus the required localized qubit in our scheme (A single AE with two degenerate metastable states is also possible for this purpose).

### Supplementary information

In this Supplementary information we provide details about the efficiency and the fault tolerance of our long-distance quantum communication architecture. We also describe the linear-optical robust entangler. Under photon losses which might be due to probabilistic single-photon sources, retrieve inefficiency of quantum memory and imperfections of single photon detectors, our protocol is still efficient. That is, our quantum repeater protocol with AEs and linear optics is photon-loss tolerant and the time needed to create a remote entangled pair scales polynomially with the communication distance.

*Single-photon polarization entangler.*—Deterministic single-photon polarization entangler is depicted in Fig 3. In ideal case (nearly ideal photon counting and quantum memory of good quality) where single photons can be created on demand and photon-number counting detectors are used to identify the Bell states, we will obtain two maximally entangled photons in the outputs  $a$  and  $b$ , conditioned on a coincidence count in two of the four detectors with a success probability  $\frac{1}{8}$ . The output state can be easily calculated as

$$\begin{aligned} |-\rangle_1 |+\rangle_{1'} |H\rangle_{2'} |V\rangle_2 &\Rightarrow \frac{1}{4} (|H\rangle_A |+\rangle_B |H\rangle_a |+\rangle_b + |V\rangle_A |-\rangle_B |V\rangle_a |-\rangle_b - |H\rangle_A |-\rangle_B |H\rangle_a |-\rangle_b - |V\rangle_A |+\rangle_B |V\rangle_a |+\rangle_b) \\ &\Rightarrow \frac{1}{4\sqrt{2}} [-i(|H\rangle_{D_1} |H\rangle_{D_4} - |V\rangle_{D_2} |V\rangle_{D_3}) |\phi_{ab}^-\rangle_{R/L} + (|H\rangle_{D_1} |V\rangle_{D_3} + |V\rangle_{D_2} |H\rangle_{D_4}) |\phi_{ab}^+\rangle_{R/L}]. \end{aligned} \quad (3)$$

In our scheme, the four single photons are prepared from four AEs via the DLCZ scheme<sup>6</sup>, which enables controllable generation, storage and retrieval of single photons with tunable frequency, timing and bandwidth<sup>15,16,17,18</sup>. Moreover, these AE-based single photons can also be experimentally generated in a fashion heralded by a feedback mechanism which greatly suppresses two-photon events<sup>17,18</sup>. By using AE-based, heralded single photons, the present entanglement creation efficiency shows a novel memory-enhanced feature. To see this more clearly, suppose that each heralded single photon can be successfully generated with a probability  $p_{sp}$ . With the help of quantum memory being able to store these single photons for a reasonable time, the four single photons can all be prepared in parallel within an average time  $o(1/p_{sp})$  such that the successful probability of entanglement creation is  $o(p_{sp})$ ; without quantum memory, the successful probability will be  $o(p_{sp}^4)$ . Note that the probability of emitting two photons by any AE is  $o(p_{sp}^2)$  and can thus be neglected for sufficient small  $p_{sp}$ .

However, current AE-based single photon sources<sup>15,16,17,18</sup> are probabilistic as the retrieve efficiency of single photons from AEs is not perfect; the probability is determined by the retrieve efficiency  $p_r$ . Moreover, the mostly used single photon detectors cannot distinguish between one and more than one detected photons (The visible light photon counter has the capability to do this with 99% accuracy<sup>30</sup>). Due to these imperfections, the output state in  $a$  and  $b$  is not a pure state but a mixed entangled state. Suppose that the AE-based single photon sources can generate single photons with probability  $p_r$ , and the detection efficiency of single photon detectors is  $\eta_1$  for one photon and  $\eta_2$  for two photons. It is easy to see that when there are 2 photons ( $\{1, 2\}, \{1, 2'\}, \{1', 2\}, \{1', 2'\}$ ) with probability  $p_r^2(1-p_r)^2$ , 3 photons ( $\{1, 1', 2\}, \{1, 1', 2'\}, \{1, 2, 2'\}, \{1', 2, 2'\}$ ) with probability  $p_r^3(1-p_r)$  and 4 photons ( $\{1, 1', 2', 2'\}$ ) with probability  $p_r^4$  retrieved from the AEs, there will be a coincidence count between two of the detectors.

Considering all these possibilities, we find that if only one of the four coincidence counts occurs, e.g.,  $D_1$  and  $D_4$  is registered, the output state in  $a$  and  $b$  is a mixed entangled state described by

$$\rho_c = p_{2c}\rho_{2c} + p'_{1c}\rho'_{1c} + p''_{1c}\rho''_{1c} + p'''_{1c}\rho'''_{1c} + p_{0c}\rho_0, \quad (4)$$

with

$$p_{2c} = \frac{p_r^4 \eta_1^2}{32 p_c}, \quad (5)$$

$$p'_{1c} = \frac{p_r^3 (1-p_r) \eta_1^2}{8 p_c}, p''_{1c} = \frac{p_r^4 \eta_1^2}{32 p_c}, p'''_{1c} = \frac{p_r^4 \eta_1 \eta_2}{64 p_c} \quad (6)$$

$$p_{0c} = \frac{p_r^4 \eta_1 \eta_2 + p_r^3 (1-p_r) (2\eta_1^2 + \eta_1 \eta_2) + 4p_r^2 (1-p_r^2) \eta_1^2}{32 p_c}, \quad (7)$$

where  $p_c = \frac{p_r^4}{64} (4\eta_1^2 + 3\eta_1 \eta_2) + \frac{p_r^3 (1-p_r)}{32} (6\eta_1^2 + \eta_1 \eta_2) + \frac{p_r^2 (1-p_r^2)}{8} \eta_1^2$  is the corresponding success probability. Here  $\rho_{2c}$  is one of the maximal entangled Bell states  $|\phi_{ab}^+\rangle_{R/L} = \frac{1}{\sqrt{2}} (|R_a\rangle|R_b\rangle + |L_a\rangle|L_b\rangle)$ , and

$$\rho'_{1c} = \frac{|R_a\rangle\langle R_a| + |L_a\rangle\langle L_a| + |R_b\rangle\langle R_b| + |L_b\rangle\langle L_b|}{4}, \quad (8)$$

$$\rho''_{1c} = \frac{(|R_a\rangle - |L_b\rangle)(\langle R_a| - \langle L_b|) + (|L_a\rangle + |R_b\rangle)(\langle L_a| + \langle R_b|)}{4}, \quad (9)$$

$$\rho'''_{1c} = \frac{(|R_a\rangle + |L_b\rangle)(\langle R_a| + \langle L_b|) + (|L_a\rangle - |R_b\rangle)(\langle L_a| - \langle R_b|)}{4}, \quad (10)$$

and  $\rho_{0c}$  is the vacuum state, which indicates that all the input photons are detected and there is no photon in the output  $a$  and  $b$ . To obtain the above results, the resulting entangled state  $|\phi_{ab}^-\rangle_{R/L}$  is changed into  $|\phi_{ab}^+\rangle_{R/L}$  by a local unitary transformation. The total time needed for this process is  $T_0 = \frac{t_0}{p_c}$ , where  $t_0$  is preparation time of single photons. After the event-ready mixed entangled state is successfully generated, it will be directed and stored into memory qubits at each communication node as discussed in the main text.

*Entanglement creation.*—When memory qubits at adjacent nodes  $i$  and  $i+1$  both have stored a polarization entangled photons, two photons stored in the up memory qubits are retrieved and subject to a Bell-state measurement (BSM) at the middle point. This entanglement swapping will create a mixed entangled state between the two down memory qubits (see Fig. 2a in the main text) described by

$$\rho_e = p_{2e}\rho_{2e} + p_{1e}\rho_{1e} + p_{0e}\rho_0, \quad (11)$$

with

$$p_{2e} = \frac{p_{2c}^2}{p_{2c}^2 + p_{1c}p_{2c} + \frac{p_{1c}^2}{4}}, \quad (12)$$

$$p_{1e} = \frac{p_{2c}p_{1c}}{p_{2c}^2 + p_{1c}p_{2c} + \frac{p_{1c}^2}{4}}, \quad (13)$$

$$p_{0e} = \frac{\frac{p_{1c}^2}{4}}{p_{2c}^2 + p_{1c}p_{2c} + \frac{p_{1c}^2}{4}}. \quad (14)$$

The success probability  $p_e = \frac{1}{2}p_r^2\eta_1^2 e^{-L_0/L_{att}}(p_{2c}^2 + p_{1c}p_{2c} + \frac{p_{1c}^2}{4})$  with  $p_{1c} = p'_{1c} + p''_{1c} + p'''_{1c}$  by considering the channel attenuation. Here  $\rho_{2e}$  is a maximally entangled state between the two down memory qubits,  $\rho_{1e} = \frac{|r_d\rangle_i\langle r_d| + |l_d\rangle_i\langle l_d| + |r_d\rangle_{i+1}\langle r_d| + |l_d\rangle_{i+1}\langle l_d|}{4}$  is a maximally mixed state denoted by  $\rho_1$  in the following and  $\rho_0$  is the vacuum state. The total time needed for this procedure is  $T_{ent} = \frac{T_0}{p_e}$ . Due to decoherence in the experiments, the maximally entangled state  $\rho_{2e}$  may also be a mixed state. For simplicity we assume  $\rho_{2e}$  is a mixed state of fidelity  $F_e$ , described by  $\rho_{2e} = F_e |\phi_{l_d r_d}^+\rangle\langle\phi_{l_d r_d}^+| + (1 - F_e)|\psi_{l_d r_d}^+\rangle\langle\psi_{l_d r_d}^+|$  of fidelity  $F_e > F_{\min}$ , where  $|\phi_{l_d r_d}^+\rangle = \frac{1}{\sqrt{2}}(|r_d\rangle_i|r_d\rangle_{i+1} + |l_d\rangle_i|l_d\rangle_{i+1})$  and  $|\psi_{l_d r_d}^+\rangle = \frac{1}{\sqrt{2}}(|r_d\rangle_i|l_d\rangle_{i+1} + |l_d\rangle_i|r_d\rangle_{i+1})$  are maximally entangled states between the two down memory qubits at nodes  $i$  and  $i+1$  (see Fig. 2a in the main text).

*Nested entanglement purification.*—To create a remote entangled pair, a nested entanglement purification is needed<sup>5,31</sup>. Here any step of purification is done with linear optics, as experimentally realized<sup>3</sup>. Suppose  $\mathcal{N} \equiv \ell/L_0 = k^z$  and  $k = 2^l$  ( $z, l$ : integer) mixed entangled pairs of fidelity  $F_e$  are created between A and  $C_1, C_1$  and  $C_2, \dots, C_{\mathcal{N}-1}$  and B by the above method. We first connect all the nodes except  $C_k, C_{2k}, \dots, C_{\mathcal{N}-k}$  by entanglement swapping (see Fig. 2b in the main text). This procedure yields  $\mathcal{N}/k$  pairs of length  $k$  (which corresponds to communication distance  $L = kL_0$ ) and fidelity  $F_k$  between A and  $C_k, C_k$  and  $C_{2k}, \dots, C_{\mathcal{N}-k}$  and B. After the  $j$ th connection, one can get a mixed entangled state

$$\rho_{s_j} = p_{2s_j}\rho_{2s_j} + p_{1s_j}\rho_1 + p_{0s_j}\rho_0, \quad (15)$$

with

$$p_{2s_j} = \frac{p_r^2\eta_1^2 p_{2s_{j-1}}^2}{2p_{s_j}} = \frac{\alpha^2}{\alpha^2 + \alpha + 1/4}, \quad (16)$$

$$p_{1s_j} = \frac{p_r^2\eta_1^2 p_{1s_{j-1}} p_{2s_{j-1}}}{2p_{s_j}} = \frac{\alpha}{\alpha^2 + \alpha + 1/4}, \quad (17)$$

$$p_{0s_j} = \frac{p_r^2\eta_1^2 p_{1s_{j-1}}^2}{8p_{s_j}} = \frac{1/4}{\alpha^2 + \alpha + 1/4}, \quad (18)$$

and  $\alpha = \frac{p_{2e}}{p_{1e}} = \frac{p_{2c}}{p_{1c}} < 1$ . The successful probability is  $p_{s_j} = \frac{p_r^2\eta_1^2}{2}(p_{2s_{j-1}}^2 + p_{1s_{j-1}}p_{2s_{j-1}} + p_{1s_{j-1}}^2/4)$ . Here the two-photon density matrix  $\rho_{2s_j}$  is  $\rho_{2s_j} = F_{s_j}|\phi^+\rangle_{s_j}\langle\phi^+| + (1 - F_{s_j})|\psi^+\rangle_{s_j}\langle\psi^+|$  of fidelity  $F_{s_j} = F_{s_{j-1}}^2 + (1 - F_{s_{j-1}})^2$ . Note that  $\rho_{s_0} = \rho_e$  is the mixed entangled state created by entanglement generation. One can find that  $p_{2s_j}, p_{1s_j}$ , and  $p_{0s_j}$  are the same for all the connection steps, which means that the probability to find two photons in the left memory qubits will not decrease with distance in the entanglement connection process. The time needed for the  $i$ th connection step fulfils the iteration formula

$$T_{s_j} = \frac{1}{p_{s_j}}[T_{s_{j-1}} + 2^{j-1}T_{cc} + T_{op}], \quad (19)$$

with  $T_{s_0} = T_{ent}$ . We have  $F_k = F_{s_l} \geq F_{\min}$  so that the resulting entangled pair can be purified by the quantum purification protocol. The total time needed after the  $l$ -th step can be estimated by

$$T_k = T_{s_l} \approx T_{ent} \prod_{j=1}^l p_{s_j}^{-1} \leq T_{ent} \prod_{j=1}^l \left(\frac{1}{2}p_r^2\eta_1^2 p_{2s_{j-1}}^2\right)^{-1} \quad (20)$$

$$= T_{ent} \left(\frac{1}{\frac{1}{2}p_r^2\eta_1^2 p_{2s_{j-1}}^2}\right)^l = T_{ent} \left(\frac{1}{p_k}\right)^{\log_2(L/L_0)}, \quad (21)$$

where  $p_k = \frac{1}{2}p_r^2\eta_1^2p_{2s_{j-1}}^2 = \frac{1}{2}p_r^2\eta_1^2(\frac{\alpha^2}{\alpha^2+\alpha+1/4})^2$  is a constant. It is easy to see that the total time scales polynomially with the connection distance.

To purify these entangled pairs, we construct  $2^K$  copies in parallel. After purification, we obtain one pair of fidelity  $\geq F_e$  on each of these new segments. After the  $j$ -th purification step, the entangled states in these new segments can be described by

$$\rho_{p_j} = p_{2p_j}\rho_{2p_j} + p_{1p_j}\rho_{1p_j} + p_{0p_j}\rho_{0p_j}, \quad (22)$$

where

$$p_{2p_j} = \frac{1}{2p_{p_j}}p_{2p_{j-1}}^2p_r^4\eta_1^2[F_{p_{j-1}}^2 + (1 - F_{p_{j-1}})^2], \quad (23)$$

$$p_{1p_j} = \frac{1}{p_{p_j}}[p_{2p_{j-1}}^2p_r^3(1 - p_r)\eta_1^2 + p_{2p_{j-1}}^2p_r^4F_{p_{j-1}}(1 - F_{p_{j-1}})\eta_1\eta_2 + \frac{1}{2}p_{1p_{j-1}}p_{2p_{j-1}}p_r^3\eta_1^2] \quad (24)$$

$$\begin{aligned} p_{0p_j} = & \frac{1}{p_{p_j}}[p_{2p_{j-1}}^2(\frac{1}{4}p_r^4F_{p_{j-1}}^2\eta_2^2 + p_r^3(1 - p_r)F_{p_{j-1}}^2\eta_1\eta_2 + p_r^2(1 - p_r)^2(F_{p_{j-1}} + 1/2)\eta_1^2 \\ & + p_r^3(1 - p_r)F_{p_{j-1}}(1 - F_{p_{j-1}})\eta_1\eta_2) + p_{2p_{j-1}}p_{1p_{j-1}}(p_r^2(1 - p_r)^2(F_{p_{j-1}} + 1/2)\eta_1^2 \\ & + p_r^3\frac{F_{p_{j-1}}}{2}\eta_1\eta_2) + p_{2p_{j-1}}p_{0p_{j-1}}p_r^2F_{p_{j-1}}\eta_1^2 + \frac{1}{8}p_{1p_{j-1}}^2p_r^2\eta_1^2]. \end{aligned} \quad (25)$$

The two-photon density matrix is  $\rho_{2p_j} = F_{p_j} |\phi^+\rangle_{p_j}\langle\phi^+| + (1 - F_{p_j}) |\psi^+\rangle_{p_j}\langle\psi^+|$  of fidelity  $F_{p_j} = \frac{F_{p_{j-1}}^2}{F_{p_{j-1}}^2 + (1 - F_{p_{j-1}})^2}$ .

The successful probability is

$$\begin{aligned} p_{p_j} = & \frac{1}{2}p_{2p_{j-1}}^2p_r^4\eta_1^2[F_{p_{j-1}}^2 + (1 - F_{p_{j-1}})^2] + [p_{2p_{j-1}}^2p_r^3(1 - p_r)\eta_1^2 + p_{2p_{j-1}}^2p_r^4F_{p_{j-1}}(1 - F_{p_{j-1}})\eta_1\eta_2 + \\ & \frac{1}{2}p_{1p_{j-1}}p_{2p_{j-1}}p_r^3\eta_1^2] + [p_{2p_{j-1}}^2(\frac{1}{4}p_r^4F_{p_{j-1}}^2\eta_2^2 + p_r^3(1 - p_r)F_{p_{j-1}}^2\eta_1\eta_2 + p_r^2(1 - p_r)^2(F_{p_{j-1}} + 1/2)\eta_1^2 \\ & + p_r^3(1 - p_r)F_{p_{j-1}}(1 - F_{p_{j-1}})\eta_1\eta_2) + p_{2p_{j-1}}p_{1p_{j-1}}(p_r^2(1 - p_r)^2(F_{p_{j-1}} + 1/2)\eta_1^2 + p_r^3\frac{F_{p_{j-1}}}{2}\eta_1\eta_2) \\ & + p_{2p_{j-1}}p_{0p_{j-1}}p_r^2F_{p_{j-1}}\eta_1^2 + \frac{1}{8}p_{1p_{j-1}}^2p_r^2\eta_1^2], \end{aligned} \quad (26)$$

and the time needed to implement these procedures satisfies the iteration formula

$$T_{p_j} = \frac{1}{p_{p_j}}[T_{p_{j-1}} + T_{op} + 2^l T_{cc}].$$

We also have  $T_{p_0} = T_{s_1}$  and  $\rho_{p_0} = \rho_{s_1}$ . In order to see clear how the time  $T_{p_j}$  and the probability  $p_{2p_j}$  changes during the purification process, for simplicity, we assume the detection efficiency  $\eta_1 = \eta_2 = \eta$ , the retrieve efficiency  $p_r$  is 1, and we also approximate the fidelity  $F = 1$  for convenience.

Under these assumptions, we have

$$p_{2p_j} = \frac{4p_{2p_{j-1}}^2}{6p_{2p_{j-1}}^2 + 8p_{2p_{j-1}}p_{1p_{j-1}} + 8p_{2p_{j-1}}p_{0p_{j-1}} + p_{1p_{j-1}}^2}, \quad (27)$$

$$p_{1p_j} = \frac{4p_{2p_{j-1}}p_{1p_{j-1}}}{6p_{2p_{j-1}}^2 + 8p_{2p_{j-1}}p_{1p_{j-1}} + 8p_{2p_{j-1}}p_{0p_{j-1}} + p_{1p_{j-1}}^2}, \quad (28)$$

$$p_{0p_j} = \frac{2p_{2p_{j-1}}^2 + 4p_{2p_{j-1}}p_{1p_{j-1}} + 8p_{2p_{j-1}}p_{0p_{j-1}} + p_{1p_{j-1}}^2}{6p_{2p_{j-1}}^2 + 8p_{2p_{j-1}}p_{1p_{j-1}} + 8p_{2p_{j-1}}p_{0p_{j-1}} + p_{1p_{j-1}}^2}, \quad (29)$$

and the successful probability is

$$p_{p_j} = \frac{3}{4}p_{2p_{j-1}}^2\eta^2 + p_{1p_{j-1}}p_{2p_{j-1}}\eta^2 + p_{2p_{j-1}}p_{0p_{j-1}}\eta^2 + \frac{1}{8}p_{1p_{j-1}}^2\eta^2. \quad (30)$$

Through some calculations, we find that  $\frac{p_{2p_j}}{p_{1p_j}} = \alpha$ ,  $p_{2p_j} \approx \frac{\alpha^2}{2^j - 1}$ , and the time needed for  $K$ -th purification step is  $T_{p_K} \approx T_k \prod_{j=1}^K p_{p_j}^{-1} < T_k \prod_{j=1}^K (\frac{3}{4}p_{2p_{j-1}}^2\eta^2)^{-1} \approx T_k \frac{2^{K(K-1)}}{(\frac{3\alpha^4\eta^2}{4})^K}$ , which also scales polynomially with the purification steps.

We iterate the nested purification procedure until the  $z$ -th level, and finally we get a remote entangled pair described by

$$\rho_f = p_{2f}\rho_{2f} + p_{1f}\rho_1 + p_{0f}\rho_0. \quad (31)$$

The probability that one can find two photons in the remote entangled memory qubits is  $p_{2f} \approx \frac{\alpha^2}{2^{K-1}}$ , and  $\rho_{2f}$  is a mixed entangled state of fidelity  $F_f > F_e$ . The total time needed in these procedures is  $T_f < T_{ent}(\frac{1}{p_k})^{Lz}(\frac{2^{K^2+2(K-1)}}{(\frac{3\alpha^4\eta^2}{4})^K(\alpha^2+\alpha+1/4)})^z = T_{ent}(\frac{1}{p_k})^{\log_2 \ell/L_0}(\frac{2^{K^2+2(K-1)}}{(\frac{3\alpha^4\eta^2}{4})^K(\alpha^2+\alpha+1/4)})^{\log_k \ell/L_0}$ , which also scales polynomially with distance. We thus show that our quantum repeater protocol is totally fault-tolerant.

For all practical purposes of using  $\rho_{AB}$ , the presence of  $\rho_1$  and  $\rho_0$  merely reduces the efficiency in all quantum information protocols (e.g., quantum cryptography) relying on two-photon coincidences between A and B. This is the price one has to pay when using poor photon detections and poor memories.

In ideal cases, we have  $p_c = \frac{1}{8}$ ,  $p_k = \frac{1}{2}$ , and  $p_e = \frac{1}{2}e^{-L_0/L_{att}}$ . Assuming the communication time  $T_{cc} > T_0$ , the total time needed for the whole nested purification procedure can be estimated by (see the main text)  $T_{tot} \sim 2T_{cc}p_e^{-1}p_k^{-zL} \prod_{m=1}^z \prod_{i=1}^K p_{mi}^{-1}$ , where  $p_{mi}$  is the success probability of the  $i$ th purification for the  $m$ th nesting level.

High-efficiency (> 99%) photon counting based on the AE-based quantum memory technique<sup>24,25</sup> will eliminate significant noises in our protocol. The improvement of the retrieve efficiency of single photons from AEs<sup>32</sup> will also improve the quality of the AE-based single photon sources used in our scheme. Thus, the future advance on AE-based photon counting and quantum memory will push quantum communication into a longer and longer length scales.

- 
- \* Electronic address: zbchen@ustc.edu.cn  
† Electronic address: jian-wei.pan@physi.uni-heidelberg.de  
<sup>1</sup> Bouwmeester, D. *et al.* Experimental quantum teleportation. *Nature* **390**, 575-579 (1997).  
<sup>2</sup> Pan, J.-W., Bouwmeester, D., Weinfurter, H. & Zeilinger, A. Experimental entanglement swapping: Entangling photons that never interacted. *Phys. Rev. Lett.* **80**, 3891-3894 (1998).  
<sup>3</sup> Pan, J.-W., Gasparoni, S., Ursin, R., Weihs G. & Zeilinger, A. Experimental entanglement purification of arbitrary unknown states. *Nature* **423**, 417-422 (2003).  
<sup>4</sup> Gisin, N., Ribordy, G., Tittel, W. & Zbinden, H. Quantum cryptography. *Rev. Mod. Phys.* **74**, 145-195 (2002).  
<sup>5</sup> Briegel, H.-J., Dür, W., Cirac, J.I. & Zoller, P. Quantum repeaters: The role of imperfect local operations in quantum communication. *Phys. Rev. Lett.* **81**, 5932-5935 (1998).  
<sup>6</sup> Duan, L.-M., Lukin, M., Cirac, J.I., & Zoller, P. Long-distance quantum communication with atomic ensembles and linear optics. *Nature* **414**, 413-418 (2001).  
<sup>7</sup> Childress, L., Taylor, J.M., Sørensen, A.S. & Lukin, M.D. Fault-tolerant quantum communication based on solid-state photon emitters. *Phys. Rev. Lett.* **96**, 070504 (2006).  
<sup>8</sup> van Loock, P. *et al.* Hybrid quantum repeater using bright coherent light. *Phys. Rev. Lett.* **96**, 240501 (2006).  
<sup>9</sup> Lukin, M.D., Yelin, S.F. & Fleischhauer, M. Entanglement of atomic ensembles by trapping correlated photon states. *Phys. Rev. Lett.* **84**, 4232-4235 (2000).  
<sup>10</sup> Fleischhauer, M. & Lukin, M.D. Dark-state polaritons in electromagnetically induced transparency. *Phys. Rev. Lett.* **84**, 5094-5097 (2000).  
<sup>11</sup> A. Kuzmich *et al.* Generation of nonclassical photon pairs for scalable quantum communication with atomic ensembles. *Nature* **423**, 731-734 (2003).  
<sup>12</sup> van del Wal C.H. *et al.* Atomic memory for correlated photon states. *Science* **301**, 196-200 (2003).  
<sup>13</sup> Matsukevich, D.N. *et al.* Entanglement of a photon and a collective atomic excitation. *Phys. Rev. Lett.* **96**, 030405 (2006).  
<sup>14</sup> Chou, C.W. *et al.* Measurement-induced entanglement for excitation stored in remote atomic ensembles. *Nature* **438**, 828-832 (2005).  
<sup>15</sup> Chanelière, T. *et al.* Storage and retrieval of single photons transmitted between remote quantum memories. *Nature* **438**, 833-836 (2005).  
<sup>16</sup> Eisaman, M.D. *et al.* Electromagnetically induced transparency with tunable single-photon pulses. *Nature* **438**, 837-841 (2005).  
<sup>17</sup> Matsukevich, D.N. *et al.* Deterministic single photons via conditional quantum evolution. *Phys. Rev. Lett.* **97**, 013601 (2006).  
<sup>18</sup> Chen, S. *et al.* A deterministic and storable single-photon source based on quantum memory. Preprint available at <<http://xxx.lanl.gov/quant-ph/0607036>> (2006).  
<sup>19</sup> Bennett, C.H. *et al.* Teleporting an unknown quantum state via dual classical and Einstein-Podolsky-Rosen channels. *Phys. Rev. Lett.* **73**, 3081-3084 (1993).  
<sup>20</sup> Żukowski, M., Zeilinger, A., Horne, M.A. & Ekert, A. "Event-ready-detectors" Bell experiment via entanglement swapping. *Phys. Rev. Lett.* **71**, 4287-4290 (1993).  
<sup>21</sup> Bennett, C.H. *et al.* Purification of noisy entanglement and faithful teleportation via noisy channels. *Phys. Rev. Lett.* **76**, 722-725 (1995).

- <sup>22</sup> Holman, K.W., Hudson, D.D., Ye, J. & Jones, D.J. Remote transfer of a high-stability and ultralow-jitter timing signal. *Opt. Lett.* **30**, 1225-1227 (2005).
- <sup>23</sup> Simon, C. & Irvine, W.T.M. Robust long-distance entanglement and a loophole-free Bell test with ions and photons. *Phys. Rev. Lett.* **91**, 110405 (2003).
- <sup>24</sup> Imamoglu, A. High efficiency photon counting using stored light. *Phys. Rev. Lett.* **89**, 163602 (2002).
- <sup>25</sup> James, D.F.V. & Kwiat, P.G. Atomic-vapor-based high efficiency optical detectors with photon number resolution. *Phys. Rev. Lett.* **89**, 183601 (2002).
- <sup>26</sup> Felinto, D., Chou, C.W., de Riedmatten, H., Polyakov, S.V. & Kimble, H.J. Control of decoherence in the generation of photon pairs from atomic ensembles. *Phys. Rev. A* **72**, 053809 (2005).
- <sup>27</sup> Dantan, A. *et al.* Long-lived quantum memory with nuclear atomic spins. *Phys. Rev. Lett.* **95**, 123002 (2005).
- <sup>28</sup> Peng, C.Z. *et al.* Experimental free-space distribution of entangled photon pairs over 13km: Towards satellite-based global quantum communication. *Phys. Rev. Lett.* **94**, 150501 (2005).
- <sup>29</sup> Raussendorf, R. & Briegel, H.J. A One-way quantum computer. *Phys. Rev. Lett.* **86**, 5188-5191 (2001).
- <sup>30</sup> Waks, E., Inoue, K., Diamanti, E., & Yamamoto, Y. High efficiency photon number detection for quantum information processing. Preprint available at <<http://xxx.lanl.gov/quant-ph/0308054>> (2003).
- <sup>31</sup> Dür, W., Briegel, H.-J., Cirac, J.I. & Zoller, P. Quantum repeaters based on entanglement purification. *Phys. Rev. A* **59**, 169-181 (1999).
- <sup>32</sup> Gorshkov, A.V., André, A., Fleischhauer, M., Sørensen, A.S., & Lukin, M.D. Optimal storage of photon states in optically dense atomic media. Preprint available at <<http://xxx.lanl.gov/quant-ph/0604037>> (2006).

**Acknowledgements** This work was supported by National NSF of China, the Chinese Academy of Sciences, the European Commission (a Marie Curie fellowship and a Marie Curie Excellence grant), the Alexander von Humboldt Foundation, and SCALA.